Theoretical Investigation of Structural and Electronic Properties of Conjugated Polymers Based on Fluorene, Carbazole, Dibenzofuran and Dibenzothiophene Oligomers

1. Geometries and Electronic Properties of Monomer

The ground-state geometries of all the monomers were fully optimized using the density functional theory (B3LYP and BH&HLYP) calculations. The optimized bond lengths inside the structure of fluorene, carbazole, dibenzofuran and dibenzothiophene monomers were considered and are summarized in Figure 28 and 28. The fluorene, carbazole, dibenzofuran and dibenzothiophene geometries under study with B3LYP and BH&HLYP methods were compared to gain the best structure for studying the electronic and optical properties. Combining B3LYP and BH&HLYP methods shows that the bond lengths from B3LYP calculations are longer than the distances from BH&HLYP calculations, as it can be seen from Figure 29. It is indicated that the effect of exchange correlation, B3LYP (20% of HF exchange) and BH&HLYP (50% of HF exchange), of density functional theory and quality of the basis set were considered.

In Figure 30, it sees that the ground-state geometry of different substitutions atom are slightly shorter than that of biphenyl. Comparing these data with the optimized geometries obtained, the results observed that the presence the different substitution atom does significantly affect the equilibrium geometry of the structures. It is interesting to point out that by substituting a carbon atom by nitrogen, oxygen and sulfur atom in the hetero-aromatic dimeric species quite remarkable changes are observed regarding the steric effects. Accordingly, the inter-ring distance (*R4*) (see in Figure 28) of fluorene, carbazole, dibenzofuran and dibenzothiophene monomers are shorter than experimental data about 0.02 Å (*R4* = 1.507 Å, (Almenningen *et al.*, 1985). As expected, the fluorene, carbazole, dibenzofuran and dibenzothiophene monomer units create π-conjugates in structures. Furthermore, the monomers of carbazole, dibenzofuran and dibenzothiophene monomers are slightly more π-conjugated than fluorene and biphenyl, respectively, due to the electron donor properties of the nitrogen, oxygen and sulfur substitution atoms. This clearly indicates that the increase of substituting nitrogen, oxygen and sulfur atoms by carbon in the hetero-aromatic for bifluorene molecule compared to carbazole, dibenzofuran and dibenzothiophene do not significantly affect the structure of the monomers. The electronic nature of the substituent is seen to play a key role on the preferred structure and properties of the dimers.

(a) (b)

Figure 28 Numbering of bond distance of (a) biphenyl and (b) fluorene (R= >CH_2), carbazole (R= >NH), dibenzofuran (R= >O) and dibenzothiophene (R= >S) monomers.

For a better understanding of the the excitation energies of fluorene (FL), carbazole (Cz), dibenzofuran (DBZF) and dibenzothiophene (DBZTh) monomers based on the first excited state with significant oscillator strength (a π-π* transition) were studied. The vertical excitation energies from ZINDO and TDDFT methods using several optimized geometries and available experimental data are shown in Table 9 and 10. The electronic properties in terms of excitation energy (E_{ex}) and oscillator strength (*f*) were then calculated.

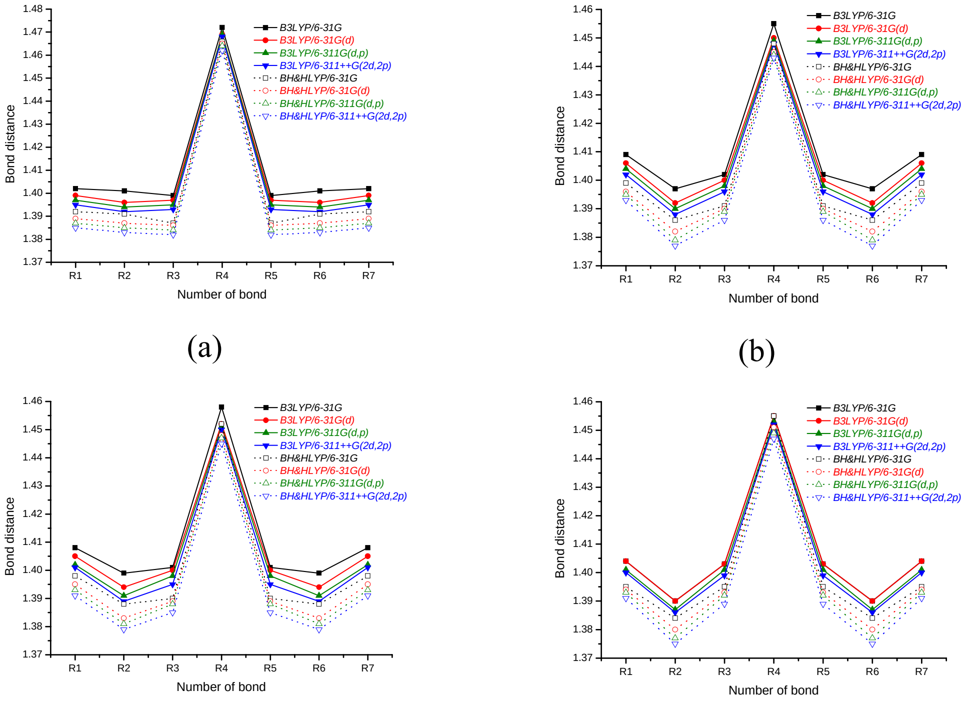

(a) (b)

(c) (d)

Figure 29 Comparison of geometrical parameters of (a) fluorene, (b) carbazole, (c) dibenzofuran and (d) dibenzothiophene monomers in the ground state from B3LYP and BH&HLYP method.

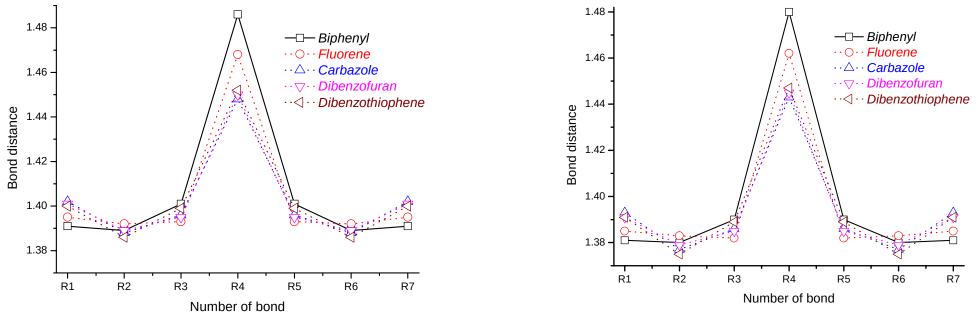

(a) (b)

Figure 30 Comparison of geometrical parameters of fluorene, carbazole, dibenzofuran and dibenzothiophene monomers obtained from (a) B3LYP and (b) BH&HLYP methods at 6-311++G(2d,2p) basis set.

Table 9 Calculated and experimental first excitation energies of fluorene (FL), carbazole (Cz), dibenzofuran (DBZF) and dibenzothiophene (DBZTh) monomers from B3LYP optimized geometries.

Methods		Excitation energy (eV)			
Excited	Optimization	FL	Cz	DBF	DBTh
ZINDO	B3LYP/6-31G	4.188	3.919	4.143	4.189
	B3LYP/6-31G(d)	4.209	3.930	4.146	4.189
	B3LYP/6-311G(d,p)	4.226	3.942	4.160	4.202
	B3LYP/6-311++G(2d,2p)	4.238	3.954	4.174	4.213
TD-B3LYP/6-31G	B3LYP/6-31G	4.753	4.213	4.582	4.290
	B3LYP/6-31G(d)	4.779	4.236	4.609	4.290
	B3LYP/6-311G(d,p)	4.800	4.252	4.626	4.305
	B3LYP/6-311++G(2d,2p)	4.815	4.265	4.641	4.315
TD-B3LYP/6-31G(d)	B3LYP/6-31G	4.650	4.129	4.509	4.201
	B3LYP/6-31G(d)	4.675	4.150	4.533	4.201
	B3LYP/6-311G(d,p)	4.695	4.165	4.550	4.215
	B3LYP/6-311++G(2d,2p)	4.709	4.178	4.5645	4.224
TD-B3LYP/6-311G(d,p)	B3LYP/6-31G	4.544	4.050	4.441	4.101
	B3LYP/6-31G(d)	4.567	4.070	4.464	4.101
	B3LYP/6-311G(d,p)	4.587	4.085	4.480	4.114
	B3LYP/6-311++G(2d,2p)	4.601	4.098	4.495	4.123
TD-B3LYP/ 6-311++G(2d,2p)	B3LYP/6-31G	4.416	3.962	4.372	4.003
	B3LYP/6-31G(d)	4.438	3.980	4.391	4.003
	B3LYP/6-311G(d,p)	4.457	3.994	4.407	4.016
	B3LYP/6-311++G(2d,2p)	4.450	4.006	4.421	4.024
TD-B3LYP/cc-pVDZ	B3LYP/6-31G	4.578	4.061	4.452	4.111
	B3LYP/6-31G(d)	4.601	4.082	4.476	4.111
	B3LYP/6-311G(d,p)	4.622	4.096	4.492	4.124
	B3LYP/6-311++G(2d,2p)	4.636	4.109	4.507	4.134
Experimental		4.23[a] 4.19[b]	3.81[a] 3.62[b]	4.24	

[a] Absorption spectrum on vapor phase. [b] Absorption spectrum on crystal phase (Marchese *et al.,* 1980).

Table 10 Calculated and experimental first excitation energies of fluorene (FL), carbazole (Cz), dibenzofuran (DBZF) and dibenzothiophene (DBZTh) monomers from BH&HLYP optimized geometries.

Methods		Excitation energy (eV)			
Excited	Optimization	FL	CZ	DBZF	DBZTh
ZINDO	BH&HLYP/6-31G	4.259	3.979	4.214	4.262
	BH&HLYP/6-31G(d)	4.280	3.988	4.209	4.254
	BH&HLYP/6-311G(d,p)	4.292	3.997	4.219	4.264
	BH&HLYP/6-311++G(2d,2p)	4.305	3.979	4.234	4.276
TD-B3LYP/ 6-31G	BH&HLYP/6-31G	4.836	4.285	4.657	4.347
	BH&HLYP/6-31G(d)	4.861	4.308	4.684	4.355
	BH&HLYP/6-311G(d,p)	4.877	4.320	4.699	4.368
	BH&HLYP/6-311++G(2d,2p)	4.893	4.285	4.715	4.380
TD-B3LYP/ 6-31G(d)	BH&HLYP/6-31G	4.729	4.129	4.580	4.265
	BH&HLYP/6-31G(d)	4.753	4.150	4.605	4.261
	BH&HLYP/6-311G(d,p)	4.768	4.165	4.619	4.273
	BH&HLYP/6-311++G(2d,2p)	4.783	4.178	4.634	4.284
TD-B3LYP/ 6-311G(d,p)	BH&HLYP/6-31G	4.620	4.117	4.511	4.163
	BH&HLYP/6-31G(d)	4.643	4.137	4.534	4.159
	BH&HLYP/6-311G(d,p)	4.658	4.149	4.548	4.170
	BH&HLYP/6-311++G(2d,2p)	4.673	4.117	4.564	4.181
TD-B3LYP/ 6-311++G(2d,2p)	BH&HLYP/6-31G	4.488	4.024	4.438	4.066
	BH&HLYP/6-31G(d)	4.509	4.042	4.457	4.057
	BH&HLYP/6-311G(d,p)	4.522	4.053	4.470	4.068
	BH&HLYP/6-311++G(2d,2p)	4.570	4.024	4.485	4.078
TD-B3LYP/ cc-pVDZ	BH&HLYP/6-31G	4.655	4.128	4.522	4.170
	BH&HLYP/6-31G(d)	4.678	4.148	4.546	4.169
	BH&HLYP/6-311G(d,p)	4.693	4.160	4.560	4.181
	BH&HLYP/6-311++G(2d,2p)	4.708	4.128	4.5753	4.192
Experimental		4.23[a]	3.81[a]	4.24	
		4.19[b]	3.62[b]		

[a] Absorption spectrum on vapor phase. [b] Absorption spectrum on crystal phase (Marchese *et al.,* 1980).

In Table 11 and 12, it can be seen that ZINDO calculations based on B3LYP/6-311G(d,p) and B3LYP/6-311++G(2d,2p) geometry for fluorene, carbazole and dibenzofuran monomers (4.20, 3.92, 4.50 and 4.20 eV, respectively) give good prediction of the excitation energies for the S_1 transition with experimental data (4.19-4.23, 3.62-3.81 and 4.24 eV, respectively). For TDDFT calculations, it is also possible to calculate the excitation energies. Because, the application of TD-B3LYP/6-311++G(2d,2p) at B3LYP/6-311G(d,p), B3LYP/6-311++G(2d,2p) and BH&HLYP/6-311++G(2d,2p) basis sets are in agreement with the experimental data in the range of 0.3 eV for all cases. From the limitation of computer time, it can select to use B3LYP/6-311G(d,p) geometry as well as geometries obtain from B3LYP/6-311++G(2d,2p) and BH&HLYP/6-311++G(2d,2p) for calculating the excitation energy. Therefore, it can use ZINDO and TD-B3LYP/6-311++G(2d,2p)//B3LYP/6-311G(d,p) level of theory to describe the excitation transitions of fluorene, carbazole, dibenzofuran and dibenzothiophene monomers in Table 11 and 12.

Table 11 Excitation energies (E$_{ex}$(eV)), oscillator strengths (*f*), and wave function composition (wf) for the low singlet electronic states of of fluorene (FL), carbazole (Cz), dibenzofuran (DBF) and dibenzothiophene (DBTh) monomers computed by ZINDO//B3LYP/6-311++G(2d,2p).

State	ZINDO//B3LYP/6-311++G(2d,2p)				Experiment[a]	
	Symmetry	wf	E$_{ex}$	*f*	State	E$_{ex}$
	(FL)					
S$_1$	B$_2$	H→L(82%)	4.238	0.4319	B$_2$	4.23
S$_2$	A$_1$	H-1→L(37%), H→L+1(48%)	4.322	0.0001	A$_1$	4.43
S$_3$	B$_2$	H-2→L(20%), H→L+2(57%)	4.443	0.0331	A$_1$	4.72
S$_4$	A$_1$	H-2→L+1(17%), H-1→ L+2 (25%), H→L+3(44%)	5.261	0.0182	A$_1$	5.21
S$_5$	B$_2$	H-2→L(54%), H→L+2(31%)	5.497	0.1792	-	-
	(Cz)					
S$_1$	A$_1$	H-1→L(59%), H→L+1(32%)	3.954	0.0219	A$_1$	3.76
S$_2$	B$_2$	H-2→L(76%)	4.139	0.2550	B$_2$	4.24
S$_3$	B$_2$	H-2→L(18%), H-1→ L+1(18%), H-1→L+3(11%), H→L+2(43%)	4.503	0.0000	B$_2$	4.85
S$_4$	B$_2$	H-1→L+1(63%), H→L(16%)	5.051	0.0000	A$_1$	5.04
S$_5$	A$_1$	H-2→L(11%), H-1→ L+2(50%), H→L+3(28%)	5.078	0.0061	A$_1$	5.35
	(DBZF)					
S$_1$	B$_2$	H→L(81%)	4.174	0.3889	A$_1$	4.24
S$_2$	A$_1$	H-1→L(45%), H→L+1(42%) H-2→L(19%), H→L+2(55%)	4.181	0.0034	B$_2$	4.46
S$_3$	B$_2$	H-2→L+1(15%), H-1→ L+2(30%), H→L+3(44%)	4.507	0.0343	A$_1$	4.64
S$_4$	A$_1$	H-2→L+2(14%), H-1→ L+1(71%)	5.209	0.0702	A$_1$	5.58
S$_5$	B$_2$	H-1→L(47%), H→L+1(48%)	5.418	0.0098	-	-
	(DBZTh)					
S$_1$	B$_2$	H→L(86%)	4.213	0.4261	-	-
S$_2$	A$_1$	H-1→L(47%), H→L+2(40%)	4.216	0.0029	-	-
S$_3$	B$_2$	H-2→L+1(24%), H→ L+2(55%)	4.430	0.0054	-	-
S$_4$	A$_1$	H-2→L+1(15%), H-1→ L+2(37%), H→L+3(29%)	5.204	0.0764	-	-
S$_5$	B$_2$	H-2→L(18%), H-2→ L+2(12%), H-1→L+1(48%)	5.432	1.0922	-	-

[a](Marchese *et al.*, 1980).

Table 12 Excitation energies (E_{ex}(eV)), oscillator strengths (*f*), and wave function composition (wf) for the low singlet electronic states of of fluorene (FL), carbazole (Cz), dibenzofuran (DBF) and dibenzothiophene (DBTh) monomers computed by TD(B3LYP/6-311++G(2d,2p)//B3LYP/6-311++G(2d,2p).

	TD(B3LYP/6-311++G(2d,2p)//B3LYP/6-311++G(2d,2p)				Experiment[a]	
State	Symmetry	wf	E_{ex}	*f*	State	E_{ex}
	(FL)					
S_1	B_2	H-2→L(43%), H→L(43%), H→L+1(38%)	4.47	0.1547	B_2	4.23
S_2	B_2	H→L(38%), H→L+1(45%)	4.67	0.2854	A_1	4.43
S_3	A_1	H-1→L(62%), H→L+3(34%)	4.84	0.0072	A_1	4.72
S_4	A_2	H→L+2(98%)	5.24	0.0000	A_1	5.21
S_5	B_1	H→L+4(99%)	5.48	0.0105	-	-
	(Cz)					
S_1	A_1	H→L(87%)	4.00	0.0285	A_1	3.76
S_2	B_2	H-1→L(71%), H→L+2(19%)	4.42	0.1438	B_2	4.24
S_3	B_1	H→L+1(98%)	4.74	0.0000	B_2	4.85
S_4	A_2	H-1→L+1(99%)	5.09	0.0000	A_1	5.04
S_5	B_1	H→L+3(97%)	5.17	0.0061	A_1	5.35
	(DBZF)					
S_1	A_1	H-1→L(81%), H→L+1(14%)	4.42	0.0275	A_1	4.24
S_2	B_2	H→L(77%)	4.55	0.2994	B_2	4.46
S_3	B_2	H-2→L(49%), H→L+3(40%)	5.21	0.0343	A_1	4.64
S_4	A_1	H-2→L(49%), H→L+1(40%)	5.40	0.0702	A_1	5.58
S_5	B_2	H→L+2(98%)	5.48	0.0000	-	-
	(DBZTh)					
S_1	A_1	H→L(88%)	4.02	0.0238	-	-
S_2	B_2	H-1→L(67%), H→L(21%)	4.51	0.1121	-	-
S_3	A_2	H→L+3(86%), H→L+6(9%)	4.80	0.0000	-	-
S_4	A_1	H-1→L+2(15%), H→ L+1(77%)	4.89	0.0146	-	-
S_5	B_2	H-2→L(15%), H-1→ L+1(60%), H→L+2(19%)	4.89	0.0096	-	-

[a] (Marchese *et al.*, 1980).

To look at the details of the electronic transitions, the five lowest dipole-allowed excitation energies and oscillator strengths of each monomers were calculated at ZINDO and TD-B3LYP/6-311++G(2d,2p)//B3LYP/6-311G(d,p) level of calculations. In Table 11 and 12, it can see that the application of ZINDO and TD-B3LYP/6-311++G(2d,2p)//B3LYP/6-311G(d,p) gives quantitative results for the first singlet excitation energies that agree with the experimental data. Compared with the available experimental excitation energies for FL, Cz and DBF, the average deviation of the calculated excitation energies is only 0.2 eV. Both calculations can provide relatively accurate predictions of vertical excitation energies for fluorene (FL), carbazole (Cz), dibenzofuran (DBF) and dibenzothiophene (DBTh) monomers. Therefore, the ZINDO and TD-B3LYP/6-311++G(2d,2p)//B3LYP/6-311G(d,p) methods are considered to be the most suitable approaches to estimate the absorption energy, and the results were employed to investigate the details of the different states of electronic transitions. The other methods gave differences in the range of 0.3-0.5 eV.

From the data in Table 11 and 12, it was found that for fluorene (FL) and dibenzofuran (DBZF) monomers, the S_1 excitation as indicated by large oscillator strengths. For carbazole (Cz) and dibenzothiophene (DBZTh) monomers, the mainly transitions are S_2 excitation. On the other hand, the other electronic transitions of each compound possess very small oscillator strengths and therefore, these can be considered as forbidden transitions. The S_1 excitation of fluorene (FL) and dibenzofuran (DBZF) monomers correspond mainly to the promotion of an electron from the highest occupied molecular orbital (HOMO) to the lowest unoccupied molecular orbital (LUMO) (H→L). In contrast, for carbazole (Cz) and dibenzothiophene (DBTh) monomers, the S_2 excitation corresponds mainly to the promotion of an electron from the (HOMO-1) to the lowest unoccupied molecular orbital (LUMO) for carbazole (Cz) and dibenzothiophene (DBTh) monomers.

These characteristics are demonstrated in Figures 31 and 32 which describe the HOMO and LUMO transitions of monomer units obtain from ZINDO and TD-B3LYP/6-311++G(2d,2p)//B3LYP/6-311++G(2d,2p) calculations. From these Figures, it can be observed how the frontier electronic levels of the monomer are affected by the incorporation of different monomer units. The same comparison can be done for the HOMO and LUMO of fluorene which turns out to be similar to the HOMO and LUMO of dibenzofuran. Carbazole is similar to dibenzothiophene. This suggests that the pairs fluorene/dibenzofuran and carbazole/dibenzothiophene should have similar characteristics of their lowest excitation. For the result, the same comparison can be done for the HOMO and LUMO of fluorene that is similar to the HOMO and LUMO of dibenzofuran. Carbazole is similar to dibenzothiophene. This suggests that fluorene to dibenzofuran and carbazole to dibenzothiophene should have similar characteristics for their lowest excitation. The ordering and electronic configurations of the orbital calculated agree with previous theoretical studies for fluorene, carbazole and dibenzofuran. However, no previous study has been done on dibenzothiophene.

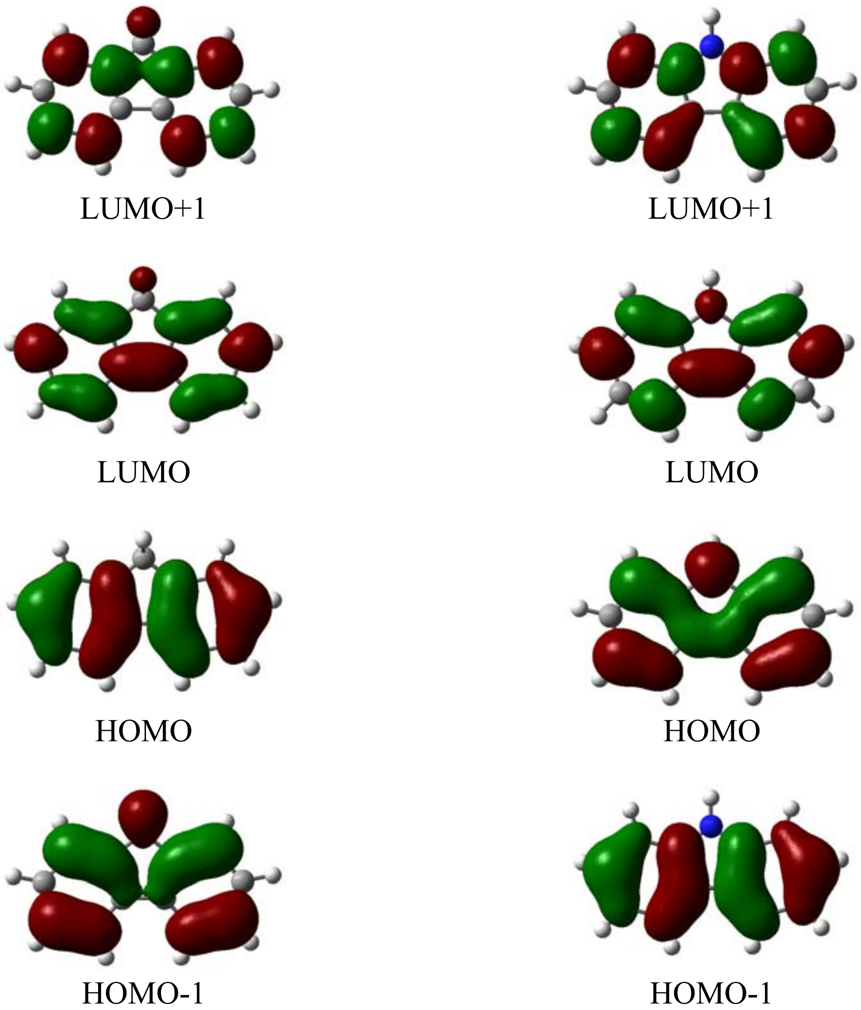

Figure 31 Calculated HOMO and LUMO of fluorene, and carbazole. Depicted are two isosurfaces of equal values but opposite sign.

LUMO+1 LUMO+1

LUMO LUMO

HOMO HOMO

HOMO-1 HOMO-1

Dibenzofuran Dibenzothiophene

Figure 32 Calculated HOMO and LUMO of dibenzofuran, and dibenzothiophene. Depicted are two isosurfaces of equal values but opposite sign.

2. Structural Geometries of Oligomer

The dimers of fluorene $(FL)_2$, carbazole $(Cz)_2$, dibenzofuran $(DBZF)_2$ and dibenzothiophene $(DBZTh)_2$, were illustrated in Table 13. The energy barriers of biphenyl (BP) has lower than the dimers of fluorene $(FL)_2$, carbazole $(Cz)_2$, dibenzofuran $(DBZF)_2$ and dibenzothiophene $(DBZTh)_2$. At all levels of description, and in agreement with previous ab initio investigations, the anti-gauche conformation is the energetically preferred structure of fluorine-based (Poolmee *et al.*, 2005; Sriwichitkamol *et al.*, 2006) and carbazole-based molecules (Yang *et al.*, 2006; Belletete *et al.*, 2004). It is indicated that all molecules are more stable in a twist configuration.

From Figure 33, it can be seen, the lowest energy conformation of fluorene, carbazole, dibenzofuran, and dibenzothiophene dimer molecules are very similar. There are two local minima with the syn-gauche and anti-gauche forms. The results indicate that the dimers of fluorene $(FL)_2$, carbazole $(Cz)_2$, dibenzofuran $(DBZF)_2$ and dibenzothiophene $(DBZTh)_2$ are nonplanar in their ground electronic states. The torsional energy curves are close to that obtained for biphenyl by using the same level of calculations. Accordingly, the inter-ring distances between both monomers are slightly shorter. Whereas, bond torsion angles of both monomers are not differently compared with biphenyl. This clearly indicates that the increase of the conjugation length observed for fluorene, carbazole, dibenzofuran, and dibenzothiophene dimer molecules compared to biphenyl does not significantly affect the conformation of the molecule.

Table 13 Energetic (kcal/mol) of stationary points in dimer structures of fluorine (FL)$_2$, carbazole (Cz)$_2$, dibenzofuran (DBZF)$_2$, and dibenzothiophene (DBZTh)$_2$ molecules relative to the planar anti conformers. (Values in parentheses are torsional angles in degrees at the local minimum).

Methods	syn	syn-gauche	perpendicular	anti-gauche	anti
(BP)					
B3LYP/6-31G	1.864	0.0 (42.7)	2.552	0.0 (137.3)	1.864
B3LYP/6-31G(d)	2.007	0.0 (41.9)	2.423	0.0 (138.1)	2.007
B3LYP/6-311G(d,p)	2.082	0.0 (40.0)	1.097	0.0 (140.0)	2.082
B3LYP/6-311++G(2d,2p)	1.860	0.0 (41.0)	1.850	0.0 (139.0)	1.860
(Cz)$_2$					
B3LYP/6-31G	2.373	0.120	2.854	0.0 (142.7)	2.185
B3LYP/6-31G(d)	2.518	0.115	2.835	0.0 (142.0)	2.166
B3LYP/6-311G(d,p)	2.535	0.111	2.151	0.0 (140.1)	2.327
B3LYP/6-311++G(2d,2p)	2.240	0.115	2.097	0.0 (141.0)	2.020
(FL)$_2$					
B3LYP/6-31G	1.986	0.034	2.944	0.0 (143.3)	1.972
B3LYP/6-31G(d)	2.115	0.020	2.785	0.0 (142.7)	2.103
B3LYP/6-311G(d,p)	2.131	0.007	2.290	0.0 (140.0)	2.120
B3LYP/6-311++G(2d,2p)	1.862	0.115	2.241	0.0 (139.8)	1.844
(DBZF)$_2$					
B3LYP/6-31G	1.870	0.077	2.967	0.0 (144.3)	1.795
B3LYP/6-31G(d)	2.085	0.028	2.740	0.0 (142.9)	2.031
B3LYP/6-311G(d,p)	2.025	0.010	2.244	0.0 (141.3)	1.974
B3LYP/6-311++G(2d,2p)	1.689	0.010	2.082	0.0 (140.5)	1.642
(DBZTh)$_2$					
B3LYP/6-31G	1.946	0.068	2.884	0.0 (143.9)	1.877
B3LYP/6-31G(d)	2.166	0.027	2.665	0.0 (142.6)	2.108
B3LYP/6-311G(d,p)	2.098	0.067	2.071	0.0 (140.8)	2.040
B3LYP/6-311++G(2d,2p)	1.697	0.115	1.922	0.0 (140.1)	1.641

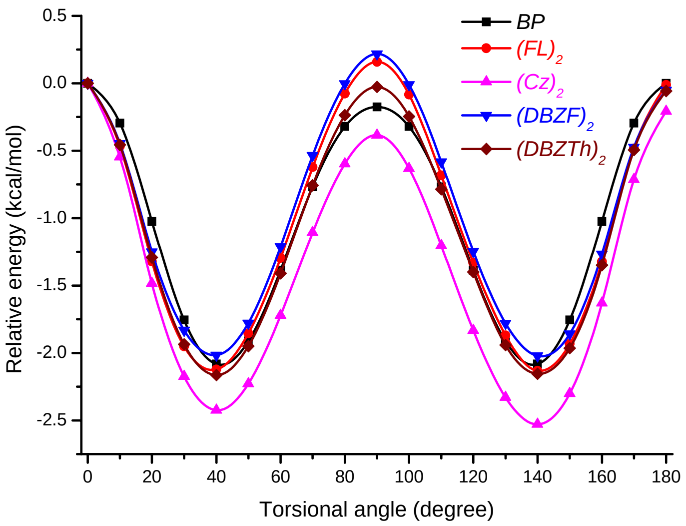

(a)

Figure 33 Torsional potential of fluorene $(FL)_2$, carbazole $(Cz)_2$, dibenzofuran $(DBZF)_2$ and dibenzothiophene $(DBZTh)_2$ dimers as obtained from B3LYP/6-311G(d,p) calculation.

Optimized ground-state geometries of fluorene $(FL)_N$, carbazole $(Cz)_N$, dibenzofuran $(DBZF)_N$ and dibenzothiophene $(DBZTh)_N$ (see Figure 20) oligomers have been calculated by using B3LYP/6-311G(d,p) method. Calculated bond distances inner the structures of monomer units and dihedral angles between subunits were considered. In Tables 14 the bond distances in the structures for the example oligomers (N = 4) of all molecules are shown. The results of optimized structures for all oligomers show that the oligomers of $(FL)_4$, $(Cz)_4$, $(DBF)_4$ and $(DBTh)_4$ molecules have similar conformation. All molecules show nonplanar structures. The dihedral angle of $(FL)_4$, $(Cz)_4$, $(DBF)_4$ and $(DBTh)_4$ molecules are about 140^o. The inter-ring distance between the subunits of $(FL)_4$, $(Cz)_4$, $(DBF)_4$ and $(DBTh)_4$ molecules are 1.485, 1.487, 1.486 and 1.485 Å, respectively. This geometry is very close to that obtained for biphenyl using the same level of calculation (Almenningen *et al.*, 1985). The ground-state geometry of all molecules is slightly less twisted than that of biphenyl (see Table 14). Accordingly, the inter-ring distance ($R_{C\text{-}C}$) are slightly shorter ($R_{C\text{-}C}$ = 1.507 Å) (Almenningen *et al.*, 1985). As expected, the different atom bridging of poly(para-phenylene) unit create steric hindrance in structures. Comparing these data with the optimized geometries obtained, the results observed that the presence the different atom of bridging of poly(para-phenylene) does significantly affect the equilibrium geometry of the structures.

Table 14 Equilibrium geometrical parameters of oligomers (N=4) in the ground state.

$R_{C\text{-}C}$ (Å)	$(FL)_4$	$(Cz)_4$	$(DBZF)_4$	$(DBZTh)_4$
R1	1.414	1.406	1.410	1.408
R2	1.389	1.395	1.384	1.391
R3	1.416	1.425	1.412	1.413
R4	1.468	1.452	1.455	1.456
R5	1.417	1.426	1.412	1.413
R6	1.389	1.395	1.384	1.391
R7	1.414	1.407	1.410	1.408
R8	1.485	1.487	1.486	1.485
R9	1.414	1.407	1.410	1.408
R10	1.389	1.395	1.384	1.391
R11	1.417	1.426	1.412	1.413
R12	1.468	1.452	1.455	1.456
R13	1.416	1.425	1.412	1.413
R14	1.389	1.395	1.384	1.391
R15	1.414	1.406	1.410	1.408
Torsional angle	143.3	142.8	144.2	144.0

3. HOMO-LUMO and Lowest Excitation Energies

It will be useful to examine the highest occupied orbitals and the lowest virtual orbitals for these oligomers and polymers because the relative ordering of the occupied and virtual orbitals provides a reasonable qualitative indication of the excitation properties and of the ability of electron or hole-transport. Because the first dipole-allowed electron transitions, as well as the strongest electron transitions with largest oscillator strength, correspond almost exclusively to the promotion of an electron from HOMO to LUMO. It is well-known that the band gap of the polymer is the orbital energy difference between the highest occupied molecular orbital (HOMO) and the lowest unoccupied molecular orbital (LUMO), when $N = \infty$. Our HOMO-LUMO gaps are obtained from density functional theory (DFT) calculations. The negative of HOMO energies ($-\varepsilon_{HOMO}$) and HOMO-LUMO gaps of the oligomers, and the extrapolated energy of $(FL)_N$, $(Cz)_N$, $(DBZF)_N$ and $(DBZTh)_N$ molecules are presented in Table 15. There is a good linear relation (about $r^2 = 0.99$) between the HOMO-LUMO gap and the inverse chain length.

In Table 15, the HOMO-LUMO gaps of real polymer can be extrapolate to the infinite chain length to get 3.24, 3.31, 3.32 and 3.34 eV to $(FL)_N$, $(Cz)_N$, $(DBZF)_N$ and $(DBZTh)_N$, respectively. The HOMO-LUMO gaps (Δ_{H-L}) are close to the experiment data, 3.25-3.30 eV to $(FL)_N$ and 3.24 eV to $(Cz)_N$. Their deviations are no more than 0.1 eV. Therefore, it is desirable to obtain the useful information in the nature of the lowest singlet excited state by employing the HOMO-LUMO gap. Because the HOMO-LUMO gap is easy to get, the approach can also be used to provide valuable information on estimate band gaps of oligomers and polymers, especially treating even larger systems. However, the orbital energy difference between HOMO and LUMO is still an approximate estimate to the transition energy since the transition energy also contains significant contributions from some two-electron integrals. The real situation is that an accurate description of the lowest singlet excited state requires a linear combination of a number of excited configurations.

From Table 15 it can be seen that the HOMO energies of $(DBZF)_N$ (-5.50 eV) and $(DBZTh)_N$ (-5.58 eV) are a higher than of $(FL)_N$ (-5.18 eV) and of $(Cz)_N$ (-5.11 eV), indicating that the presence of a heteroatom with different electronegativity has significantly improved the hole injection properties of the polymers. This is attributed to the fact that the HOMOs are mainly localized on (FL), (Cz), (DBZF) and (DBZTh) parts, and the presence of a heteroatom with different electronegativity significantly results in the large increase of the HOMO energies, whereas the LUMO energies are slightly increase on average of 0.27 eV, compared with $(FL)_N$ (-1.94 eV) and $(Cz)_N$ (-1.80 eV), suggesting the ability to accept the electron under $(FL)_N$ and $(Cz)_N$. This is reasonable, because the HOMO shows an interring antibonding character and the LUMO shows an interring bonding character, and the variation of torsional angles should have larger effects on the LUMO. Indeed, the increase in the dihedral angles induced by the presence of the electron-donating moiety carbazole should reduce the bonding character between the two subunits and thus destabilize the LUMO. Although there are some deviations between the experimental data and calculated results with respect to the HOMO and LUMO energies, these have the same trend as both HOMO and LUMO energies in $(DBZF)_N$ and $(DBZTh)_N$. There are higher than those in $(FL)_N$ and $(Cz)_N$, due to the presence of electronegative difference heteroatom, oxygen and sulfur atoms, in units have significantly improved the hole injection properties of the polymers.

The performance of TD-B3LYP/6-311G(2d,2p) method, for accurate prediction of the lowest vertical excitations of the $(FL)_N$, $(Cz)_N$, $(DBZF)_N$ and $(DBZTh)_N$ oligomers, compared to the results obtained by ZINDO method and available experimental data are shown in Table 15. Comparing to experimental excitation energies available for $(FL)_N$ and $(Cz)_N$ (2.88-2.97 and 3.83 eV, respectively (Bouchard, 2003; Belletete, 2004; Huang, 2002)), it can be seen that TD-B3LYP/6-311G(2d,2p) calculation give excellent prediction of the excitation energies for the S_1 transition (2.90 and 3.07 eV, respectively). Whereas the ZINDO method provide similar results with TD-B3LYP/6-311G(2d,2p) calculation of about 0.2 eV and gave difference of about 0.2 eV compared to experimental data. However, the TD-B3LYP/6-311G(2d,2p) calculation can provide relatively accurate predictions of vertical excitation energies for all oligomers. Compared with the available experimental excitation energies for $(FL)_N$ and $(Cz)_N$, the average deviation of the calculated excitation energies is only 0.1 eV. Therefore, the TD-B3LYP/6-311G(2d,2p) method is considered to be the most suitable approach to estimate the absorption energy, and it was employed to investigate the details of the different states of electronic transitions (see in Table 16).

The calculated vertical excitation energies and oscillator strengths for the most relevant five singlet excited states in $(FL)_4$, $(Cz)_4$, $(DBZF)_4$ and $(DBZTh)_4$ molecules are listed in Table 16. It shows that the first excitation $S_0 \rightarrow S_1$ electronic transition appears to have the highest intensity as determined by its large oscillator strength (f). The lowest lying singlet excited state is strongly optically allowed and dominated by a configuration in which an electron is excited from the highest occupied molecular orbital (HOMO) to the lowest unoccupied orbital (LUMO). On the other hand, the S_2, S_3 and S_4 electronic transitions of each compound possess very small oscillator strengths and therefore, these low probability transitions.

The contour plots of HOMO and LUMO orbitals of $(FL)_N$, $(Cz)_N$, $(DBZF)_N$ and $(DBZTh)_N$ molecules were plotted and shown in Figure 34 as an example. As shown in Figure 34, in general, the electronic cloud distributing in $(FL)_N$, $(Cz)_N$, $(DBZF)_N$ and $(DBZTh)_N$ molecules are similar and all the frontier orbitals spread over the whole π-conjugated backbone. There is antibonding between the bridge atoms of the inter-ring, and there is bonding between the bridge carbon atom and its conjoint atoms of the intra-ring in the HOMO. On the contrary, there is bonding in the bridge single bond of the inter-ring and the antibonding between the bridge atom and its neighbor of the intra-ring in the LUMO. In general, the HOMO possesses an antibonding character between the subunits. This may explain the nonplanarity observed for these oligomers in their ground states. On the other hand, the LUMO of all the oligomers generally shows a bonding character between the two adjacent subunits. This implies that the singlet excited state involving mainly the promotion of an electron from the HOMO to the LUMO should be more planar.

Table 15 Lowest TD-B3LYP/6-311G(2d,2p), ZINDO excitation energies, the negative of HOMO energies ($-\varepsilon_{HOMO}$) and HOMO-LUMO gaps of all oligomers based on /B3LYP/6-311G(d,p) geometry, all in eV.

Oligomer	TD-B3LYP/6-311G(2d,2p)	ZINDO	$-\varepsilon_{HOMO}$	Δ_{H-L}
(FL)$_N$				
N=2	3.86	3.74	5.60	4.14
N=3	3.53	3.54	5.45	3.84
N=4	3.38	3.46	5.39	3.70
N=5	3.28	3.42	5.35	3.60
	$(r^2=0.9997)$	$(r^2=0.9978)$	$(r^2=0.9995)$	$(r^2=0.9997)$
N=∞	2.90	3.19	5.18	3.24
Experimental[a, b]	2.88, 2.97		-	3.25-3.30
(Cz)$_N$				
N=2	3.59	3.71	5.54	4.19
N=3	3.49	3.53	5.40	3.89
N=4	3.34	3.45	5.33	3.75
N=5	3.25	3.40	5.29	3.66
	$(r^2=0.9999)$	$(r^2=0.9992)$	$(r^2=0.9996)$	$(r^2=0.9997)$
N=∞	3.07	3.19	5.11	3.31
Experimental[c]	3.17		5.25	3.25
(DBZF)$_N$				
N=2	3.81	3.70	5.87	4.19
N=3	3.48	3.51	5.74	3.89
N=4	3.33	3.43	5.68	3.75
N=5	3.24	3.38	5.65	3.67
	$(r^2=0.9994)$	$(r^2=0.9989)$	$(r^2=0.9979)$	$(r^2=0.9992)$
N=∞	2.85	3.16	5.50	3.32
Experimental	-		-	-
(DBZTh)$_N$				
N=2	3.80	3.72	5.93	4.22
N=3	3.50	3.52	5.81	3.91
N=4	3.35	3.44	5.75	3.78
N=5	3.28	3.39	5.73	3.70
	$(r^2=0.9995)$	$(r^2=0.9976)$	$(r^2=0.9957)$	$(r^2=0.9981)$
N=∞	2.92	3.17	5.58	3.34
Experimental	-		-	-

[a](Bouchard *et al.*, 2003)
[b](Belletete *et al.*, 2004)
[c](Huang *et al.*, 2002)

Table 16 Excitation energies (E(eV)), oscillator strengths (*f*), and wave function composition for the low singlet electronic states of $(FL)_4$, $(Cz)_4$, $(DBZF)_4$ and $(DBZTh)_4$ molecules computed by TD-B3LYP/6-311G(2d,2p) //B3LYP/6-311G(d,p).

Electronic transitions	E_{ex}	*f*	Wave function composition
$(FL)_4$			
$S_0 \rightarrow S_1$	3.38	2.916	H→L(90%)
$S_0 \rightarrow S_2$	3.83	0.006	H-1→L(72%), H→L+1(-17%)
$S_0 \rightarrow S_3$	3.84	0.001	H→L+1(76%), H-1→L(20%)
$S_0 \rightarrow S_4$	4.17	0.584	H-1→L+1(85%), H→L+2(12%)
$S_0 \rightarrow S_5$	4.18	0.136	H-2→L(20%), H→L+2(47%), H-1→L+2(-17%)
$(Cz)_4$			
$S_0 \rightarrow S_1$	3.59	2.769	H→L(90%)
$S_0 \rightarrow S_2$	3.67	0.001	H-4→L(72%)
$S_0 \rightarrow S_3$	3.68	0.028	H-5→L(80%)
$S_0 \rightarrow S_4$	3.76	0.012	H-3→L(55%), H-2→L+1(16%), H-1→L(15%)
$S_0 \rightarrow S_5$	3.76	0.010	H-3→L+1(18%), H-2→L(69%)
$(DBZF)_4$			
$S_0 \rightarrow S_1$	3.33	2.882	H→L(90%)
$S_0 \rightarrow S_2$	3.77	0.000	H-1→L(58%), H→L+1(38%)
$S_0 \rightarrow S_3$	3.78	0.013	H-1→L(-34%), H→L+1(53%)
$S_0 \rightarrow S_4$	4.03	0.027	H-6→L(61%), H→L+2(-11%)
$S_0 \rightarrow S_5$	4.10	0.138	H-6→L(15%), H-4→L(33%), H-3→L+1(10%), H-1→ L+1(13%), H→L+2(10%)
$(DBZTh)_4$			
$S_0 \rightarrow S_1$	3.35	2.894	H→L (90%)
$S_0 \rightarrow S_2$	3.66	0.002	H-4→L (73%)
$S_0 \rightarrow S_3$	3.67	0.029	H-5→L (82%)
$S_0 \rightarrow S_4$	3.73	0.017	H-3→L (59%), H-2→L+1 (17%), H-1→L (14%)
$S_0 \rightarrow S_5$	3.73	0.010	H-3→L+1 (17%), H-2→L (71%)

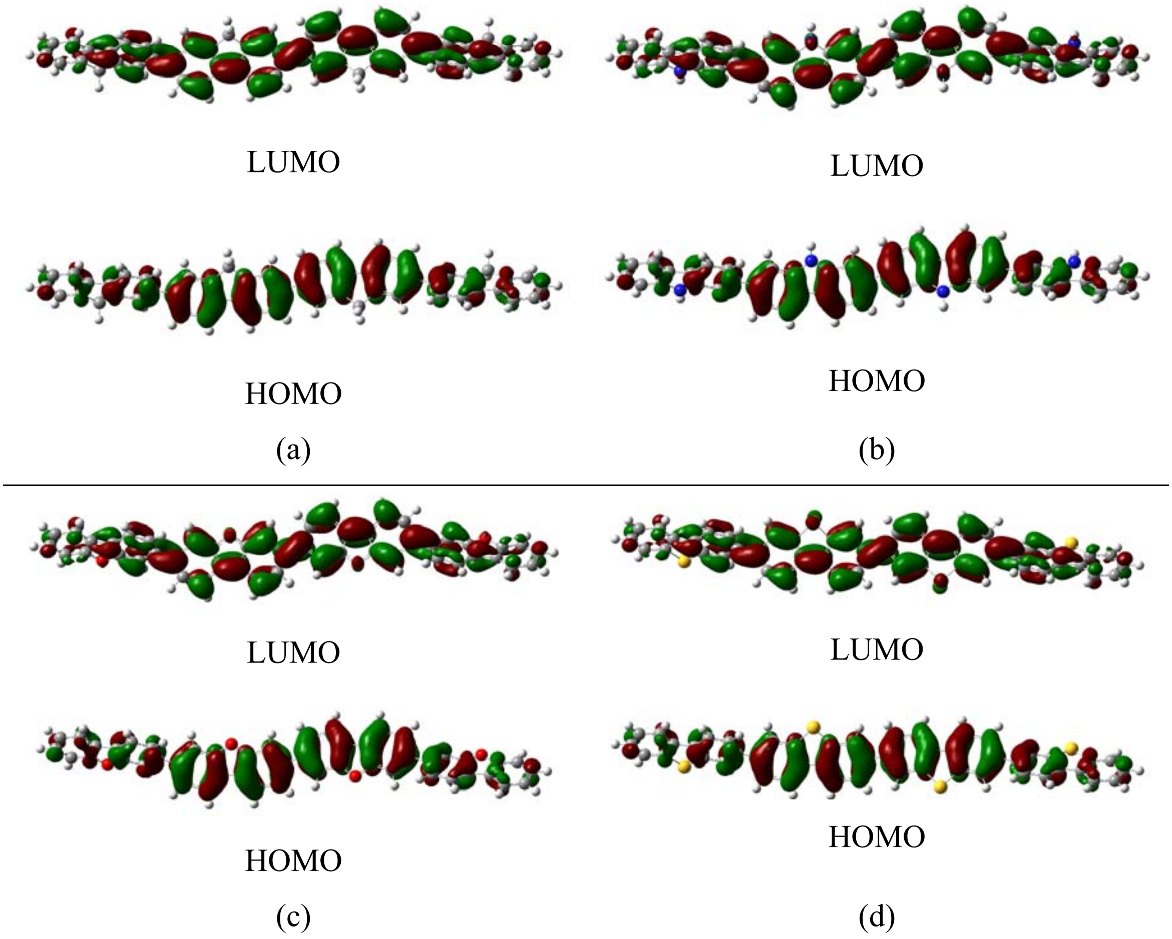

Figure 34 HOMO and LUMO of fluorene $(FL)_4$, carbazole $(Cz)_4$, dibenzofuran $(DBZF)_4$ and dibenzothiophene $(DBZTh)_4$ oligomers as obtained from B3LYP/6-311G(d,p) calculation.